Estimation of the input parameters in the Ornstein-Uhlenbeck neuronal model

Susanne Ditlevsen*
Department of Biostatistics, Panum Institute, University of Copenhagen, Blegdamsvej 3, 2200 N, Denmark

Petr Lansky†
Institute of Physiology, Academy of Sciences of the Czech Republic, Videnska 1082, 142 20 Prague 4, Czech Republic
(Received 17 August 2004; published 21 January 2005)

The stochastic Ornstein-Uhlenbeck neuronal model is studied, and estimators of the model input parameters, depending on the firing regime of the process, are derived. Closed expressions for the Laplace transforms of the first two moments of the normalized first-passage time through a constant boundary in the suprathreshold regime are derived, which is used to define moment estimators. In the subthreshold regime, the exponentiality of the first-passage time is utilized to characterize the input parameters. In the threshold regime and for the Wiener process approximation, analytic expressions for the first-passage-time density are used to derive the maximum-likelihood estimators of the parameters. The methods are illustrated on simulated data under different conditions, including misspecification of the intrinsic parameters of the model. Finally, known approximations of the first-passage-time moments are improved.

DOI: 10.1103/PhysRevE.71.011907 PACS number(s): 87.19.La, 87.10.+e, 05.40.−a, 02.50.−r

I. INTRODUCTION

A wide range of approaches to the modeling of single neurons have been proposed in the literature. The adequacy of a model depends on the task it should perform (function) and also on the desired resemblance to biological reality (form). The leaky integrate-and-fire (LIF) model appears to be one of the most common, in both artificial neural network applications and descriptions of biological systems (see, e.g., [1–4]). This model belongs to the class of so-called single-point models, in which all the characteristics of the neuron are collapsed into a single point in space. It can be used in its deterministic version or in a stochastic version, if an apparent variability in the activity of neurons should be described. In the stochastic version, under specific assumptions [5], it coincides with the Ornstein-Uhlenbeck (OU) stochastic process and has been extensively investigated in the neuronal context. Due to the simplicity of this model, some of its features are questionable, such as unlimited membrane potential fluctuation or state-independent changes of the voltage. However, it appears as a good compromise between the tractability and realism of the model.

Neuronal models of single cells reflect the electrical properties of the membrane via electric circuit description. Such circuit models can be written in terms of a differential equation for the membrane voltage. For the LIF models the firing is not an intrinsic property of the model and a firing threshold has to be imposed. As for the deterministic models, also in stochastic models an action potential (spike) is produced when the membrane voltage exceeds the voltage threshold and it corresponds to the first-passage time for the associated stochastic process describing the voltage. The voltage is instantaneously reset to its initial value. Time intervals between action potentials are identified with experimentally observable interspike intervals (ISI's). The importance of the ISI's follows as a consequence of the generally accepted hypothesis that the information transferred within the nervous system is encoded by the timing of the action potentials.

Numerous papers investigating the OU model for constant as well as periodic input have been published [6–11]. However, papers devoted to its comparison with experimental data are relatively rare. The problem is mathematically complex, and the task is analytically solvable only for a simplified version of the OU model: namely, the Wiener process. However, the Wiener process is so simplified that any fit to data must be taken with the utmost care. The model can be used as a statistical descriptor characterizing the activity of a specific neuron under specific conditions, but it contains no information about the biophysical mechanisms responsible for the spike generation.

The verification of any model has to start with an estimation of its parameters. To derive an efficient estimation procedure based on ISI data for any model more complex than the Wiener process is not an easy task. This was shown in [12,13], where the parameters for the OU neuronal model were estimated. The methods used in these two papers were heavily based on an intensive numerical search of the data and their comparison with numerically calculated distributions of ISI's. Simultaneously, with the effort to estimate the parameters from ISI's, methods for their estimation based on continuous or discrete sampling of the membrane potential between spikes have been proposed [14,15]. Nevertheless, this is a problem for which a different type of data than ISI's has to be available and is not considered in this article.

The aim of the present contribution is to derive methods of parameter estimation based on ISI data in the OU neuronal model. We restrict ourselves to an estimation of the input parameters assuming that the intrinsic parameters are known, and the effects of misspecification of these parameters are investigated. The ISI data follow different distribu-

*Electronic address: sudi@pubhealth.ku.dk
URL: http://www.biostat.ku.dk/~sudi/
†Electronic address: lansky@biomed.cas.cz

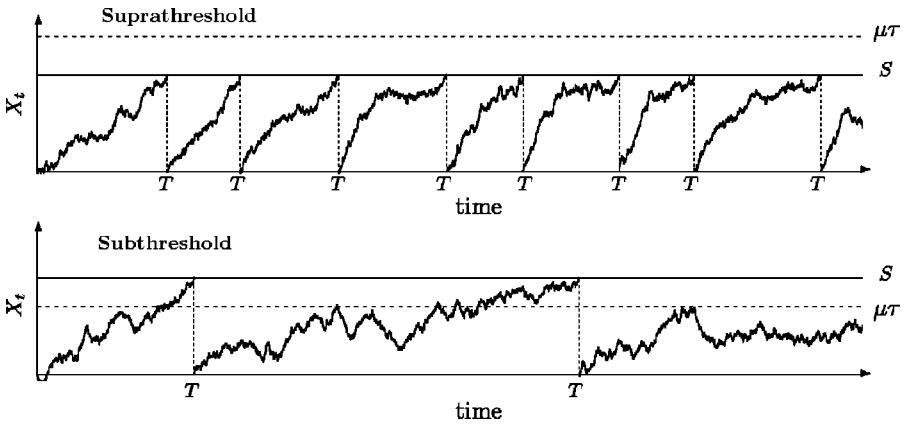

FIG. 1. Realizations of X_t (membrane potential against time, arbitrary units). When the threshold S is reached at time T, both process and time are reset to 0. The dashed line $\mu\tau$ is the asymptotic depolarization. Upper panel: suprathreshold regime. Lower panel: subthreshold regime.

tions depending on the parameters of the model, so it is natural to divide the parameter space in different regimes characterized by their qualitative behavior. Known results are used to derive estimators in some parts of the parameter space. A closed expression for the Laplace transform of the ISI, valid in a subset of the parameter space, is deduced and used for a moment estimator. The results are illustrated on simulated data from one regime and compared with the Wiener process approximation.

II. MODEL AND ITS PARAMETERS

The changes in the membrane potential between two consecutive neuronal firings are represented by a stochastic process X_t indexed by the time t. The reference level for the membrane potential is taken to be the resting potential. The initial voltage (the reset value following a spike) is assumed to be equal to the resting potential and set to zero, $X_0=x_0=0$. An action potential is produced when the membrane voltage X exceeds a voltage threshold for the first time, for simplicity assumed to be equal to a constant $S>0$. Formally, the interspike interval T is identified with the first-passage time of the threshold,

$$T = \inf\{t > 0 : X_t \geq S\}. \tag{1}$$

It follows from the model assumptions that for time-homogeneous input containing either a Poissonian or white noise only, the interspike intervals form a renewal process and the initial time can always be identified with zero. Here we consider the white noise input and X is a diffusion process. A scalar diffusion process $X=\{X_t; t\geq 0\}$ can be described by the stochastic differential equation

$$dX_t = \mu(X_t,t)dt + \sigma(X_t,t)dW_t, \tag{2}$$

where $W=\{W_t; t\geq 0\}$ is a standard Wiener process and $\mu(\cdot)$ and $\sigma(\cdot)$ are real-valued functions of their arguments called the infinitesimal mean and variance. We investigate the diffusion process (2) specified by the infinitesimal mean

$$\mu(X_t,t) = -\frac{X_t}{\tau} + \mu, \tag{3}$$

where constant μ characterizes the neuronal input and $\tau>0$ reflects spontaneous voltage decay (the membrane time constant) in the absence of input. Moreover, we consider a constant infinitesimal variance

$$\sigma(X_t,t) = \sigma, \tag{4}$$

where $\sigma>0$ is the second input parameter. The diffusion process (2) with the infinitesimal moments (3) and (4) defines the OU diffusion process:

$$dX_t = \left(-\frac{X_t}{\tau} + \mu\right)dt + \sigma dW_t, \quad X_0 = x_0 = 0. \tag{5}$$

The OU model yields the Wiener (or "perfect integrator") model in the limit of an infinitely large time constant, $\tau \to \infty$. The parameters appearing in Eqs. (1) and (5) can be divided into two groups: parameters characterizing the input, μ and σ, and intrinsic parameters τ, x_0, and S, which describe the neuron irrespectively of the incoming signal [16].

Solving either the Fokker-Planck equation or the Kolmogorov equation for Eqs. (5) yields the transition density function

$$f(x,t) = (2\pi V_t)^{-1/2}\exp\left\{-\frac{(x-M_t)^2}{2V_t}\right\}, \tag{6}$$

where

$$M_t = \mu\tau(1-e^{-t/\tau}), \tag{7}$$

$$V_t = \frac{\sigma^2\tau}{2}(1-e^{-2t/\tau}). \tag{8}$$

Hence, at each time t the transition probability density function is normal with mean M_t and variance V_t.

Two distinct firing regimes, usually called subthreshold and suprathreshold, can be established for the OU model; see Fig. 1. In the suprathreshold regime, the asymptotic mean depolarization $\mu\tau$ given by Eq. (7) is far above the firing threshold S and the ISI's are relatively regular (deterministic firing—which means that the neuron is active also in the absence of noise). In the subthreshold regime, $\mu\tau \ll S$ and firing is caused only by random fluctuations of the depolarization (stochastic or Poissonian firing). The term "Poissonian firing" indicates that when the threshold is far above the steady-state depolarization $\mu\tau$ (relatively to σ), the firing achieves characteristics of a Poisson point process [17–19]. For our purposes, let us denote the third regime, when $\mu\tau$

$\approx S$, as the threshold regime. In the specific situation $\mu\tau = S$, the first-passage-time density of the OU process across the boundary S is known [6,20]:

$$f(t) = \frac{2S \exp\left(\frac{2t}{\tau}\right)}{\sqrt{\pi\tau^3\sigma^2}\left[\exp\left(\frac{2t}{\tau}\right) - 1\right]^{3/2}} \times \exp\left\{-\frac{S^2}{\sigma^2\tau\left[\exp\left(\frac{2t}{\tau}\right) - 1\right]}\right\}. \quad (9)$$

Division of the firing regimes into three parts was already proposed in [19].

For comparison, for the Wiener process obtained as the limit when $\tau \to \infty$ in Eqs. (5), the first-passage-time density is

$$f(t) = \frac{S}{\sqrt{2\pi\sigma^2 t^3}} \exp\left\{-\frac{(S-\mu t)^2}{2\sigma^2 t}\right\}, \quad (10)$$

which is known as the inverse Gaussian distribution in the statistical literature [21,22]. It must be pointed out that the OU model differs from the Wiener model in several relevant aspects. For instance, for the OU model an equilibrium regime exists since in the limit as $t \to \infty$ the probability density (6) becomes normal with mean $\mu\tau$ and variance $\sigma^2\tau/2$. Furthermore, the crossing of the firing threshold is a sure event independently on μ, whereas for model (10), neuronal firing is a sure event if $\mu \geqslant 0$.

III. ESTIMATION OF THE INPUT PARAMETERS

The first problem one encounters when estimating parameters in the OU model from ISI data is the determination of the regime since the distribution of T is different in the three regimes, and different estimation procedures should thus be applied. In the subthreshold regime the ISI's are approximately exponentially distributed, whereas in the threshold and suprathreshold regimes the process of the first-passage times is far from being Poisson. It is not obvious how to determine the regime, but one could, e.g., perform an exponential distribution test, thus discriminating between subthreshold or others. If an exponential distribution of ISI's is rejected, the suprathreshold estimation procedure is applied. In the case it suggests that the data were generated by the process in the threshold regime by estimating $\mu \approx S/\tau$, it is finally investigated as such.

When a closed expression for the density of the first-passage-time distribution is available, maximum-likelihood estimation can be applied, and this also provides estimators of the asymptotic variance of the estimators from the inverted Fisher information evaluated at the optimum. This is the case in the threshold regime and for the Wiener process approximation, Eqs. (9) and (10). In the subthreshold regime the density is approximately exponential, which suggests the corresponding maximum-likelihood estimators. In the suprathreshold regime, where the distribution is not available, we propose a moment estimator. A representation of the Laplace transform is given by

$$E[e^{kT/\tau}] = \frac{\exp\left\{\frac{(\mu\tau)^2}{2\tau\sigma^2}\right\} D_k\left(\frac{\sqrt{2}\mu\tau}{\sqrt{\tau}\sigma}\right)}{\exp\left\{\frac{(\mu\tau - S)^2}{2\tau\sigma^2}\right\} D_k\left(\frac{\sqrt{2}(\mu\tau - S)}{\sqrt{\tau}\sigma}\right)} = \frac{H_k\left(\frac{\mu\tau}{\sqrt{\tau}\sigma}\right)}{H_k\left(\frac{(\mu\tau - S)}{\sqrt{\tau}\sigma}\right)} \quad (11)$$

for $k < 0$, where $D_k(\cdot)$ and $H_k(\cdot)$ are parabolic cylinder and Hermite functions, respectively; see [23,24]. The result can be extended to $k > 0$ in a certain part of the parameter space. Specifically, we deduce closed expressions for $k = 1$ and 2, requiring $\mu\tau > S$ (suprathreshold) and $\sigma^2 < 2(\mu\tau - S)^2/\tau$, which provides closed expressions of moment estimators. This last method is checked on simulated data sets and compared to the threshold estimation in the case when the estimation yields $\hat{\mu} < S/\tau + \varepsilon$ for some small ε and to the Wiener approximation.

The data are assumed to be n observations of T: t_i, $i = 1, \ldots, n$. The model assumes that the neuronal output forms a renewal process, so that the observations will be independent and identically distributed. Note that since we are only interested in estimating two parameters of a distribution, n does not have to be as large as if we want to estimate the functional form of the distribution of T.

A. Subthreshold regime

If $\mu\tau \ll S$, the first-passage-time density function can be approximated by an exponential distribution [17–19]

$$f(t) = \lambda \exp(-\lambda t), \quad (12)$$

where

$$\lambda = \frac{\sigma\sqrt{\pi\tau}}{S - \mu\tau} \exp\left(-\frac{(S - \mu\tau)^2}{\sigma^2\tau}\right). \quad (13)$$

It is easily seen that from this distribution it is only possible to determine μ and σ up to the parameter function $\theta = (S - \mu\tau)/\sigma\sqrt{\tau}$. Maximum likelihood yields the estimating equation

$$\frac{\hat{\theta}}{\sqrt{\pi}} \exp(\hat{\theta}^2) = \overline{t}, \quad (14)$$

where $\overline{t} = (1/n)\Sigma_{i=1}^{n} t_i$. The equation is easily solved numerically. The asymptotic variance of the estimator estimated from the inverted Fisher information evaluated at the optimum is given by

$$\mathrm{var}[\hat{\theta}] = \frac{\hat{\theta}^2}{n(1 - 2\hat{\theta}^2)^2}. \quad (15)$$

B. Threshold regime

If $\mu\tau = S$, the first-passage-time density is given by Eq. (9). In this case only σ needs to be estimated since $\mu = S/\tau$,

and it is straightforward to calculate the maximum-likelihood estimator:

$$\hat{\sigma}^2 = \frac{1}{n}\sum_{i=1}^{n} \frac{2S^2}{\tau[\exp(2t_i/\tau) - 1]}. \tag{16}$$

The asymptotic variance of the estimator calculated by the inverted Fisher information at the optimum is given by

$$\mathrm{var}[\hat{\sigma}] = \frac{\hat{\sigma}^2}{2n}. \tag{17}$$

C. Suprathreshold regime

By defining suitable martingales and applying Doob's optional-stopping theorem, it is possible to find closed expressions for the Laplace transform $E[e^{kT/\tau}]$, $k=1,2$, in the suprathreshold regime and with certain restrictions on the size of σ. These expressions can then be applied to define estimators for this parameter region. In the Appendix it is shown that

$$E[e^{T/\tau}] = \frac{\mu\tau}{\mu\tau - S}, \tag{18}$$

$$E[e^{2T/\tau}] = \frac{2(\mu\tau)^2 - \tau\sigma^2}{2(\mu\tau - S)^2 - \tau\sigma^2}, \tag{19}$$

if

$$\sigma^2 < \frac{2(\mu\tau - S)^2}{\tau}. \tag{20}$$

Condition (20) means that the asymptotic standard deviation of X_t is smaller than the distance between the threshold and the asymptotic mean of X_t. Straightforward estimators of $E[e^{T/\tau}]$ and $E[e^{2T/\tau}]$ are obtained from the empirical moments:

$$Z_1 = \hat{E}[e^{T/\tau}] = \frac{1}{n}\sum_{i=1}^{n} e^{t_i/\tau}, \tag{21}$$

$$Z_2 = \hat{E}[e^{2T/\tau}] = \frac{1}{n}\sum_{i=1}^{n} e^{2t_i/\tau}. \tag{22}$$

Moment estimators of the parameters, assuming that the data are in the allowed parameter region, are then obtained from Eqs. (18) and (19):

$$\hat{\mu} = \frac{SZ_1}{\tau(Z_1 - 1)} \tag{23}$$

and

$$\hat{\sigma}^2 = \frac{2S^2(Z_2 - Z_1^2)}{\tau(Z_2 - 1)(Z_1 - 1)^2}. \tag{24}$$

Note that the asymptotic depolarization will always be estimated to be suprathreshold ($\hat{\mu}\tau > S$) and that $0 < \hat{\sigma}^2 < 2(\hat{\mu}\tau - S)^2/\tau$. It follows from Eq. (23) that $\hat{\mu} \approx S/\tau$ if $Z_1 \approx Z_1 - 1$. In other words, if $t_i \gg \tau$ for some i, the data suggest that the model is not in the suprathreshold regime. This shows the importance of the time constant for determining the firing regimes.

D. Approximations of the ISI moments

Approximations of the mean and variance of T were proposed in [19,25] in a parameter region which corresponds to our suprathreshold regime. It is shown there that for $S=1$ and $\tau=1$,

$$E[T] \approx \ln\left(\frac{\mu}{\mu - 1}\right) - \frac{\sigma^2}{4}\left(\frac{1}{(\mu-1)^2} - \frac{1}{\mu^2}\right), \tag{25}$$

$$\mathrm{var}[T] \approx \frac{\sigma^2}{2}\left(\frac{1}{(\mu-1)^2} - \frac{1}{\mu^2}\right), \tag{26}$$

in the case $\mu - 1 \gg \sigma$. Using the exact results (18) and (19) we can refine Eqs. (25) and (26) and give exact conditions on μ and σ for the approximation to be valid. Taylor expansion of $\ln(e^T)$ to second order around $E[e^T]$ and taking expectations yields

$$\begin{aligned} E[T] &= E[\ln e^T] \\ &\approx \ln(E[e^T]) - \frac{\mathrm{var}[e^T]}{2E[e^T]^2} \\ &= \ln\left(\frac{\mu}{\mu-1}\right) - \frac{\sigma^2}{4}\left(\frac{2\mu - 1}{\mu^2[(\mu-1)^2 - \sigma^2/2]}\right). \end{aligned} \tag{27}$$

This approximation is valid if $\mu > 1$ and $\sigma < \sqrt{2}(\mu - 1)$ [condition (20) for $S=1$ and $\tau=1$]. Repeating the calculation for $[\ln(e^T)]^2$ yields

$$E[T^2] = E[(\ln e^T)^2] \approx \{\ln(E[e^T])\}^2 - \{\ln(E[e^T]) - 1\}\frac{\mathrm{var}[e^T]}{E[e^T]^2}, \tag{28}$$

so that

$$\mathrm{var}[T] \approx \frac{\sigma^2}{2}\left(\frac{2\mu - 1}{\mu^2[(\mu-1)^2 - \sigma^2/2]}\right), \tag{29}$$

ignoring higher-order terms. Approximating further in Eqs. (27) and (29) by assuming $(\mu-1)^2 - \sigma^2/2 \approx (\mu-1)^2$ yields Eqs. (25) and (26).

E. Wiener process approximation

In the simpler case, when $\tau \to \infty$ in Eqs. (5), the first-passage-time density is given by Eq. (10), and it is straightforward to calculate the maximum-likelihood estimators:

$$\hat{\mu} = \frac{S}{\bar{t}}, \tag{30}$$

$$\hat{\sigma}^2 = S^2\left(\frac{1}{n}\sum_{i=1}^{n}\frac{1}{t_i} - \frac{1}{\bar{t}}\right). \tag{31}$$

The estimators are stochastically independent and the variances are

$$\mathrm{var}[\hat{\mu}] = \frac{\hat{\sigma}^2}{nt} + \frac{2\hat{\sigma}^4}{n^2 S^2}, \tag{32}$$

$$\mathrm{var}\left[\frac{1}{\hat{\sigma}^2}\right] = \frac{2}{n\hat{\sigma}^4}; \tag{33}$$

see [21,22]. For comparison, the asymptotic variances of the estimators estimated by the inverted Fisher information evaluated at the optimum are given by $\mathrm{var}[\hat{\mu}]=\hat{\sigma}^2/nt$ and $\mathrm{var}[\hat{\sigma}^2]=2\hat{\sigma}^4/n$, which can be used as convenient approximations of Eqs. (32) and (33).

IV. EXAMPLES AND NUMERICAL RESULTS

Trajectories from the OU process in the threshold and suprathreshold regimes were simulated according to the Euler scheme with a step size of 0.01 msec for different input parameter values. The process was run until reaching a threshold S where the time was recorded. This was repeated 100 times, and on the data sets obtained, μ and σ were estimated after performing a Kolmogorov-Smirnov test of exponential distribution to test the regime. All simulated data sets were highly rejected as exponentially distributed: the highest p value was 0.0036 and the mean was less than 10^{-4}.

Three sets of simulations were run: the first to test the estimators (23) and (24), the second to evaluate the possible influence from misspecifications in the intrinsic parameters on the same estimators, and the third to compare with the estimators (30) and (31) from the Wiener process approximation. In the last two sets of simulations, also estimator (16) was applied.

In the first set of simulations the parameter values were set to $\mu=1.5$ mV/msec, $\sigma=1$ mV/$\sqrt{\text{msec}}$, $\tau=10$ msec, and $S=10$ mV. A 1000 data sets each of size 100 were generated, and on each of them μ and σ were estimated. The estimates of μ averaged 1.496 ± 0.035 mV/msec (mean±standard deviation), and the estimates of σ averaged 0.926 ± 0.127 mV/$\sqrt{\text{msec}}$. Normal quantile plots of the estimates are in Fig. 2. The estimator of μ appears nonbiased, with small variance and normal distribution, whereas the estimator of σ underestimates the correct value and is far from being normal, with a heavy tail to the right.

In the second set of simulations the influence of misspecifications in the intrinsic parameters is investigated. μ was either 1, 1.5, or 2 mV/msec, and σ was either 0.1, 1, or 1.5 mV/$\sqrt{\text{msec}}$. Five combinations of the intrinsic parameters were considered: $\tau=10$ msec and $S=8$, 10, and 12 mV, respectively, and $S=10$ mV and $\tau=8$ and 12 msec, respectively, for each of the nine combinations of input parameter values. Only μ's for which $\mu\tau \geqslant S$ were considered, which gives a total of 39 combinations. A 100 data sets were generated for each combination, and on each data set μ and σ were estimated. In the estimation procedure it was assumed that $\tau=10$ msec and $S=10$ mV. In Fig. 3 the results are summarized, where the points represent the average of the estimates for each combination of parameters.

When the intrinsic parameters are well specified (○'s on the panels), estimates of μ are superior in all cases. If S is assumed larger (=10) than the true value (=8), μ tends to be overestimated (△'s in left panel) and underestimated if S is assumed smaller (=10) than the true value (=12) (+'s in left panel). Misspecifications in τ have the opposite effect on the estimates of μ (×'s and ◇'s in left panel).

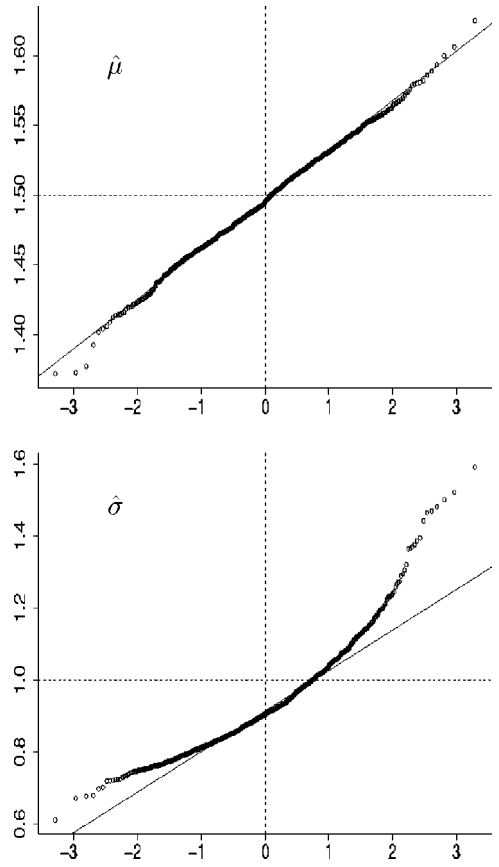

FIG. 2. Gaussian quantile plots (empirical versus theoretical quantiles) for the estimators (23) and (24) from the 1000 artificial data sets simulated with $\mu=1.5$ mV/msec, $\sigma=1$ mV/$\sqrt{\text{msec}}$, $\tau=10$ msec, and $S=10$ mV. The straight lines pass through the first and third quartiles; the horizontal lines are set at the parameter values used in the simulations.

The picture for $\hat{\sigma}$ is more complicated (right panel). As already shown in Fig. 2, $\hat{\sigma}$ seems downward biased. When σ does not fulfill condition (20) it is poorly estimated. Misspecifications in τ and S appear to have the same effects of either enlarging or reducing $\hat{\sigma}$ as on $\hat{\mu}$.

When the suprathreshold estimator (23) estimates μ to be in threshold regime—i.e., $\hat{\mu}\tau - S < \varepsilon$ for some small ε—the threshold estimator (16) for σ should be applied. This is the case for the left points in each group in right panel of Fig. 3, where the estimates (16) of σ are seen to be superior (only the case with well-specified intrinsic parameters is included). When we are far from threshold regime, the estimator (16) is very poor (some points fall above plotting region).

In the third set of simulations it was assumed that the intrinsic parameters were well specified, but two values of the time constant were considered, $\tau=10$ or 20 msec, and S was set to 10 mV. The same sets of input parameters as before were used. Estimation was performed both with suprathreshold estimation, Eqs. (23) and (24), with the Wiener

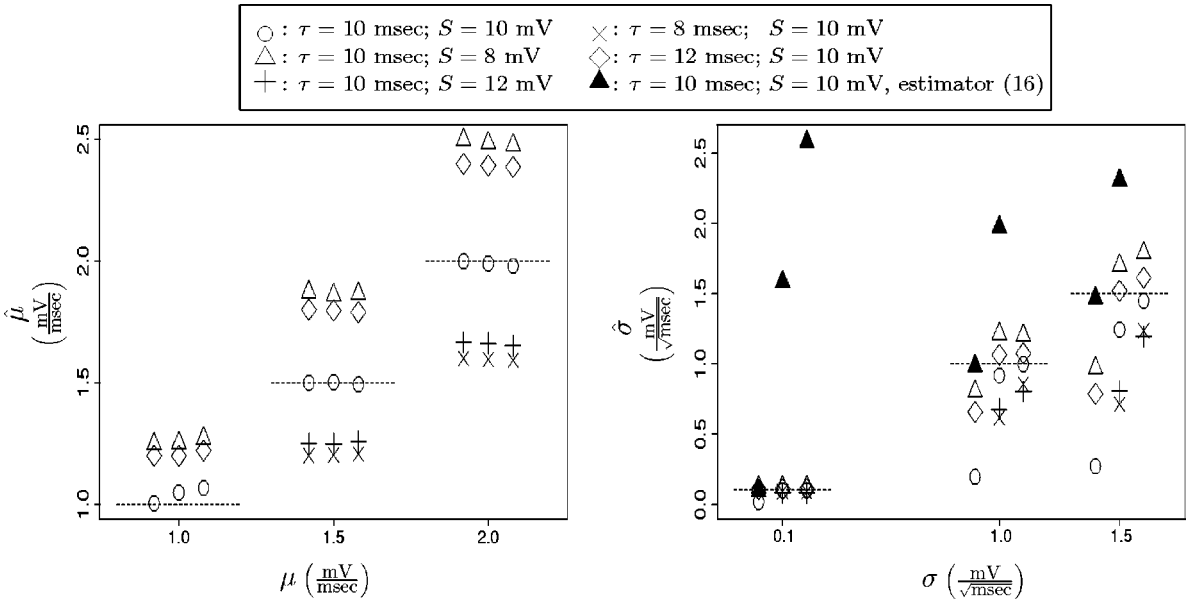

FIG. 3. Mean from 100 realizations of the estimators (23) and (24) when S and τ are misspecified. Each data set consists of 100 simulated ISI's. Left panel: estimates of μ versus correct values. For each value of μ, $\sigma=0.1$ mV/$\sqrt{\text{msec}}$ (left points), $\sigma=1.0$ mV/$\sqrt{\text{msec}}$ (middle points), and $\sigma=1.5$ mV/$\sqrt{\text{msec}}$ (right points). Right panel: estimates of σ versus correct values. For each value of σ, $\mu=1.0$ mV/msec (left points), $\mu=1.5$ mV/msec (middle points), and $\mu=2.0$ mV/msec (right points). Also estimator (16) is plotted in the right panel when S and τ are well specified (points above plotting region are missing). The dashed lines are the identity lines, indicating the best possible estimates.

process approximation, Eqs. (30) and (31), and with threshold estimation, Eq. (16). Again, 100 data sets were generated for each combination of parameters. In Fig. 4 the results are summarized, with points representing the average of estimates.

The estimator (23) of μ (○'s and △'s in left panel) is clearly superior to (30) (×'s and +'s in left panel). Not surprisingly, the Wiener process approximation improves when τ is larger, since in the limit when $\tau\to\infty$, the OU process converges to the Wiener process.

As before, the estimator (24) of σ is always poor when condition (20) is not fulfilled. The estimator (31) does not seem sensitive to the approximation and is always good, maybe except for small σ in the threshold regime. If Eq. (23)

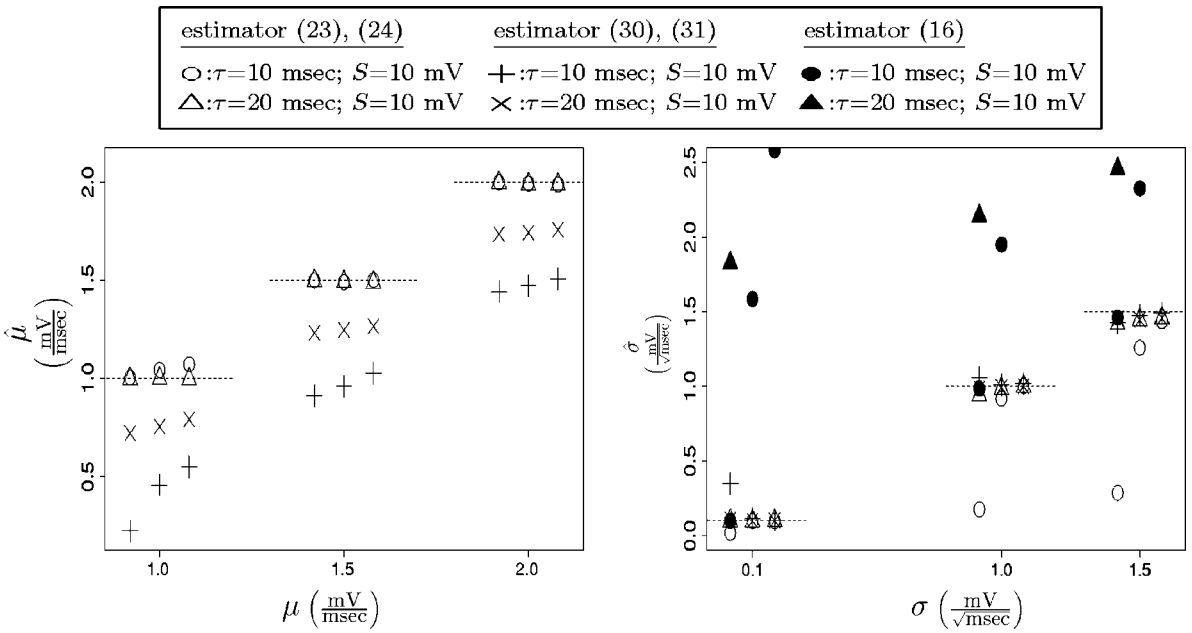

FIG. 4. Estimation assuming the full model and the Wiener approximation, respectively, on data sets simulated from the full model for different time constants. Mean from 100 realizations. Left panel: estimates of μ. Right panel: estimates of σ. Points above plotting region of estimator (16) are missing (right panel). The dashed lines are the identity lines, indicating the best possible estimates.

gives $\hat{\mu}\tau \approx S$, then Eq. (24) should not be applied. Instead, if there is confidence in the value of τ, a good choice would be Eq. (16), otherwise Eq. (31).

Simulations of trajectories in the subthreshold regime is a difficult task, and there exists a large literature on this subject [26–28]. It is not the aim of the present paper to face these problems, and only the threshold and suprathreshold regimes have been considered.

V. DISCUSSION

The distribution of the first-passage time through a constant level by an OU process has been the subject of many studies, not only in neuronal modeling [29]. In this paper we use results on moments and distributions to propose estimators of the input parameters, depending on the regime.

The main contributions of the present work are the derivation of expressions for $E[e^{T/\tau}]$ and $E[e^{2T/\tau}]$ of the first-passage time of the OU process through a constant threshold. This leads to simple and closed expressions for moment estimators of μ and σ in the suprathreshold regime and when σ is small relative to the distance between the asymptotic depolarization and the threshold. The appealing feature is that the numerical difficulties arising from the handling of the expressions given in the known results for the Laplace transform (where the exponents of the exponential function in the expectations are negative) are avoided.

The results obtained from the simulated data show that the proposed estimation procedure in the suprathreshold regime works excellently for μ. The variance parameter σ is more difficult, especially when σ is larger than the condition required for the expressions of the above-mentioned moments to be correct. We suggest estimating μ, and in case it indicates that the process is the near-threshold regime, another estimator for σ should be applied—e.g., the maximum-likelihood estimator for σ when the process is in the threshold regime or the estimator derived from the Wiener process approximation of the OU process.

In this paper only the situation where the intrinsic parameters are assumed to be known is considered. The time constant τ has shown to be crucial for the estimation, and a way of estimating also this parameter from ISI data could be the following. If σ is estimated with the Wiener process approximation (31), then Eqs. (18) and (19) with the left-hand sides substituted with Eqs. (21) and (22) would constitute a two-equation system with two unknowns (μ and τ), which could be solved numerically.

Previously, a computer-intensive method was proposed in [12] for the estimation of the same two parameters in the OU model as in this paper. Their method is based on the experimentally observed first- and second-order moments of interspike intervals and applied to interspike interval data recorded from neurons in the mesencephalic reticular formation of the cat during hypothetical sleep, slow-wave sleep stage, and wake stage. However, the numerical evaluations implicated are difficult to handle for the general researcher.

In [13] it was directly stated that the OU model does not reproduce spiking statistics of neurons in prefrontal cortex. Their analysis is based on the coefficient of variation and the skewness coefficient, which are, respectively, a measure of the spiking irregularity and a measure of the asymmetry of the interval distribution. It was found that the data are not consistent with the model if the time constant takes a value considered as standard one. The authors deduced from the finding that unless the inputs are correlated, the OU model is not adequate. This idea was further pursued in [30] where the correlation of consecutive ISIs was introduced. The authors concluded that the OU model with temporally correlated inputs may account for the data if the correlation time scale of the inputs is on the order of 100 msec. The same modeling approach was applied in [31].

The model might be too simple to reproduce the interspike intervals realistically. A natural generalization of the model was introduced simultaneously with the classical LIF model (for references see [32]). In this model the passive membrane time constant is replaced by a drive-dependent effective time constant. More specifically, drift (3) in Eq. (2) is replaced by

$$\mu(X_t,t) = -\frac{X_t}{\tau} + \mu(V_{\mathrm{E}} - X_t) + \nu(X_t - V_{\mathrm{I}}), \tag{34}$$

where $\mu > 0$ and $\nu < 0$ are new constants characterizing the input. It is obvious that now the model has an input-dependent time constant and its behavior will be different from the OU model. In addition, taking into account the variable conductance, the infinitesimal variance becomes state dependent [33]. The estimation in this type of models will be investigated elsewhere.

ACKNOWLEDGMENTS

We are grateful to Michael Sørensen for suggestions and comments on the Appendix. This work was supported by the Grant Agency of the Czech Republic Grant No. (309/02/0168), the Academy of Sciences Grant (Information Society T400110401), and the European Community's Human Potential Programme under Contract No. HPRN-CT-2000-00100, DYNSTOCH.

APPENDIX

Consider the OU model (5) for the membrane potential X at time t, with solution

$$X_t = \mu\tau - e^{-t/\tau}(\mu\tau - \omega_t), \tag{A1}$$

where $\omega_t = \sigma\int_0^t e^{s/\tau} dW_s$. We will now prove Eqs. (18) and (19) using martingales, which will be defined using the conditional moments from the OU process. In general, for a martingale M_t and a stopping time $\mathcal{T}$, we have $E[M_{\mathcal{T}\wedge t}] = E[M_0]$, where $\mathcal{T}\wedge t = \min(\mathcal{T}, t)$. For a subclase we have the stronger result (see [34], p. 221)

Doob's optional-stopping theorem. Let $\mathcal{T}$ be a stopping time and let M_t be a uniformly integrable martingale. Then $E[M_{\mathcal{T}}] = E[M_0]$.

Note that T given by Eq. (1) is a stopping time. For $k \in \mathbb{N}$, Eq. (A1) yields that $(X_t - \mu\tau)^k e^{kt/\tau} = (\omega_t - \mu\tau)^k$ so that

$E[(\omega_t-\mu\tau)^k|\omega_s]=E[(X_t-\mu\tau)^k e^{kt/\tau}|X_s]$. For $t>s$ we therefore have

$$E[(\omega_t-\mu\tau)|\omega_s]=(\omega_s-\mu\tau), \tag{A2}$$

$$E[(\omega_t-\mu\tau)^2|\omega_s]=(\omega_s-\mu\tau)^2+\frac{\tau\sigma^2}{2}(e^{2t/\tau}-e^{2s/\tau}), \tag{A3}$$

$$E[(\omega_t-\mu\tau)^4|\omega_s]=\left((\omega_s-\mu\tau)^2+\frac{3\tau\sigma^2}{2}(e^{2t/\tau}-e^{2s/\tau})\right)^2 - \frac{3\tau^2\sigma^4}{2}(e^{2t/\tau}-e^{2s/\tau})^2. \tag{A4}$$

Define the filtration $\mathcal{F}_t=\sigma(X_s;0\leqslant s\leqslant t)$, the σ algebra generated by X_s for $0\leqslant s\leqslant t$. Then the process

$$Y_t=(\mu\tau-X_t)e^{t/\tau}=\mu\tau-\omega_t \tag{A5}$$

is a martingale with respect to $\mathcal{F}_t$ by Eq. (A2) and because $E[Y_t]<\infty$ since X_t is Gaussian. Therefore $Y_t^T=Y_{T\wedge t}$, the process Y_t stopped at T, is also a martingale (see [34], p. 99). Moreover, if $\mu\tau>S$ and $\sigma^2<2(\mu\tau-S)^2/\tau$, then Y_t^T is uniformly integrable. To show this it is enough to show that $E[|Y_t^T|^p]<K$ for all t, for some $p>1$ and K a positive constant; see [34], p. 127. First define

$$\tilde{Y}_t=(\mu\tau-\omega_t)^2-\frac{\tau\sigma^2}{2}(e^{2t/\tau}-1), \tag{A6}$$

which is a martingale with respect to $\mathcal{F}_t$:

$$\begin{aligned}E[\tilde{Y}_t|\mathcal{F}_s]&=E\left[(\mu\tau-\omega_t)^2-\frac{\tau\sigma^2}{2}(e^{2t/\tau}-1)|\omega_s\right]\\&=(\mu\tau-\omega_s)^2+\frac{\tau\sigma^2}{2}(e^{2t/\tau}-e^{2s/\tau})-\frac{\tau\sigma^2}{2}(e^{2t/\tau}-1)\\&=\tilde{Y}_s,\end{aligned} \tag{A7}$$

using Eq. (A3), and that all moments of a Gaussian variable are finite, so that $E[\tilde{Y}_t]<\infty$. Therefore,

$$(\mu\tau)^2=E[\tilde{Y}_0]=E[\tilde{Y}_{T\wedge t}]=E[(\mu\tau-\omega_{T\wedge t})^2] - \frac{\tau\sigma^2}{2}E[(e^{2(T\wedge t)/\tau}-1)]. \tag{A8}$$

Put $p=2$, then

$$\begin{aligned}E[|Y_t^T|^2]&=E[(\mu\tau-\omega_{T\wedge t})^2]=(\mu\tau)^2+\frac{\tau\sigma^2}{2}E[(e^{2(T\wedge t)/\tau}-1)]\\&\leqslant(\mu\tau)^2+\frac{\tau\sigma^2}{2}E[e^{2T/\tau}]\end{aligned} \tag{A9}$$

by Eq. (A8). To give an upper bound on $E[e^{2T/\tau}]$ use Eq. (A8) again to obtain

$$\begin{aligned}(\mu\tau)^2&=E\left[(\mu\tau-X_{T\wedge t})^2e^{2(T\wedge t)/\tau}-\frac{\tau\sigma^2}{2}(e^{2(T\wedge t)/\tau}-1)\right]\\&\geqslant(\mu\tau-S)^2E[e^{2(T\wedge t)/\tau}]-\frac{\tau\sigma^2}{2}(E[e^{2(T\wedge t)/\tau}]-1),\end{aligned} \tag{A10}$$

where we have used that $(\mu\tau-X_{T\wedge t})^2>(\mu\tau-S)^2$ when $\mu\tau>S$ (suprathreshold case). Since $\sigma^2<2(\mu\tau-S)^2/\tau$, Eq. (A10) can be rearranged to

$$\frac{2(\mu\tau)^2-\tau\sigma^2}{2(\mu\tau-S)^2-\tau\sigma^2}\geqslant E[e^{2(T\wedge t)/\tau}]. \tag{A11}$$

Taking limits on both sides we obtain

$$\frac{2(\mu\tau)^2-\tau\sigma^2}{2(\mu\tau-S)^2-\tau\sigma^2}\geqslant\lim_{t\to\infty}E[e^{2(T\wedge t)/\tau}]=E[e^{2T/\tau}] \tag{A12}$$

by monotone convergence. Doob's optional-stopping theorem can therefore be applied to Y_t^T if $\mu\tau>S$ and if $\sigma^2<2(\mu\tau-S)^2/\tau$. This yields

$$\mu\tau=E[Y_0^T]=E[Y_T^T]=E[(\mu\tau-X_T)e^{T/\tau}]=(\mu\tau-S)E[e^{T/\tau}], \tag{A13}$$

which finally yields Eq. (18). To prove Eq. (19) note that from Eq. (A12) we have that in the given parameter subset $E[e^{2T/\tau}]$ is finite so that Eq. (11) can be applied, which directly yields

$$E[e^{2T/\tau}]=\frac{H_2\left(\frac{\mu\tau}{\sqrt{\tau\sigma}}\right)}{H_2\left(\frac{(\mu\tau-S)}{\sqrt{\tau\sigma}}\right)}=\frac{4\left(\frac{\mu\tau}{\sqrt{\tau\sigma}}\right)^2-2}{4\left(\frac{(\mu\tau-S)}{\sqrt{\tau\sigma}}\right)^2-2}=\frac{2(\mu\tau)^2-\tau\sigma^2}{2(\mu\tau-S)^2-\tau\sigma^2}.$$

[1] M. Arbib, *The Handbook of Brain Theory and Neural Networks*, 2nd ed. (MIT Press, Cambridge, MA, 2002).

[2] P. Dayan and L. Abbott, *Theoretical Neuroscience: Computational and Mathematical Modeling of Neural Systems* (MIT Press, Cambridge, MA, 2001).

[3] W. Gerstner and W. Kistler, *Spiking Neuron Models* (Cambridge University Press, Cambridge, England, 2002).

[4] H. Tuckwell, *Introduction to Theoretical Neurobiology* (Cambridge University Press, Cambridge, England, 1988), Vol. 2.

[5] P. Lansky, J. Theor. Biol. **107**, 631 (1984).

[6] A. Bulsara, T. Elston, C. Doering, S. Lowen, and K. Lindenberg, Phys. Rev. E **53**, 3958 (1996).
[7] P. Lansky, L. Sacerdote, and F. Tomasetti, Biol. Cybern. **73**, 457 (1995).
[8] L. Ricciardi and L. Sacerdote, Biol. Cybern. **35**, 1 (1979).
[9] H. Robinson and A. Harsch, Phys. Rev. E **66**, 061902 (2002).
[10] T. Shimokawa, K. Pakdaman, T. Takahata, S. Tanabe, and S. Sato, Biol. Cybern. **83**, 327 (2000).
[11] H. Tuckwell, F. Wan, and J. Rospars, Biol. Cybern. **86**, 137 (2002).
[12] J. Inoue, S. Sato, and L. Ricciardi, Biol. Cybern. **73**, 209 (1995).
[13] S. Shinomoto, Y. Sakai, and S. Funahashi, Neural Comput. **11**, 935 (1999).
[14] M. Habib and A. Thavaneswaran, Appl. Math. Comput. **38**, 51 (1990).
[15] P. Lansky, Math. Biosci. **67**, 247 (1983).
[16] H. Tuckwell and W. Richter, J. Theor. Biol. **71**, 167 (1978).
[17] J. Keilson and H. Ross, *Selected Tables in Mathematical Statistics* (American Mathematical Society, Providence, 1975), Vol. 3, pp. 233–327.
[18] A. Nobile, L. Ricciardi, and L. Sacerdote, J. Appl. Probab. **22**, 360 (1985).
[19] F. Wan and H. Tuckwell, J. Theor. Neurobiol. **1**, 197 (1982).
[20] L. Ricciardi, *Diffusion Processes and Related Topics in Biology* (Springer, Berlin, 1977).
[21] R. Chhikara and J. Folks, *The Inverse Gaussian Distribution: Theory, Methodology, and Applications* (Marcel Dekker, New York, 1989).
[22] M. Tweedie, Ann. Math. Stat. **28**, 362 (1957).
[23] A. Borodin and P. Salminen, *Handbook of Brownian Motion—Facts and Formulae* (Birkhauser Verlag, Basel, 2002).
[24] N. Lebedev, *Special Functions and Their Applications* (Dover, New York, 1972).
[25] C. Smith, J. Theor. Biol. **154**, 271 (1992).
[26] M. Giraudo and L. Sacerdote, Commun. Stat.-Simul. Comput. **28**, 1135 (1999).
[27] P. Lansky and V. Lanska, Comput. Biol. Med. **24**, 91 (1994).
[28] R. Mannella, Phys. Lett. A **254**, 257 (1999).
[29] S. Redner, *Guide to First-Passage Processes* (Cambridge University Press, Cambridge, England, 2001).
[30] Y. Sakai, S. Funahashi, and S. Shinomoto, Neural Networks **12**, 1181 (1999).
[31] E. Salinas and T. Sejnowski, Neural Comput. **14**, 2111 (2002).
[32] M. Richardson, Phys. Rev. E **69**, 051918 (2004).
[33] P. Lansky and V. Lanska, Biol. Cybern. **56**, 19 (1987).
[34] D. Williams, *Probability with Martingales* (Cambridge University Press, Cambridge, England, 1991).